17th World Conference on Earthquake Engineering, 17WCEE
Sendai, Japan - September 13th to 18th 2020

CATEGORIZATION OF THE FAULT PARAMETERS USED FOR STRONG MOTION PREDICTION AND THEIR ALEATORY UNCERTAINTY

K. Dan[(1)], A. Oana[(2)], M. Tohdo[(3)], H. Fujiwara[(4)], and N. Morikawa[(5)]

[(1)] *Ohsaki Research Institute, Inc., Japan, dan@ohsaki.co.jp*
[(2)] *Ohsaki Research Institute, Inc., Japan, a.oana@ohsaki.co.jp*
[(3)] *Ohsaki Research Institute, Inc., Japan, tohdo@ohsaki.co.jp*
[(4)] *National Research Institute for Earth Science and Disaster Resilience, Japan, fujiwara@bosai.go.jp*
[(5)] *National Research Institute for Earth Science and Disaster Resilience, Japan, morikawa@bosai.go.jp*

Abstract

There are 27 fault parameters needed for strong motion prediction by the Recipe of the Headquarters for Earthquake Research Promotion (2017, [1]), Japan. We categorized these fault parameters into four groups as follows.

I) parameters defined by geological, geomorphological, or seismological investigation

location and geometry of the active fault, segment for strong motion evaluation, strike, dip, rake, upper depth of the seismogenic layer, lower depth of the seismogenic layer, location of the asperities

II) parameters calculated by theoretical relationships with other parameters

seismic fault length, seismic fault width, seismic fault area, moment magnitude, averaged stress drop, averaged slip over the entire fault, asperity area, asperity stress drop, seismic moment on the asperity

III) parameters calculated by empirical relationships with other parameters

seismic moment, short-period level, averaged slip on the asperity, area of each asperity, slip velocity time function, f_{max}, rupture propagation velocity

IV) parameters set by assumption

hypocenter, rupture propagation mode

We also judged whether each parameter in the categories III and IV has an epistemic uncertainty or aleatory uncertainty as follows: seismic moment (epistemic and aleatory), short-period level (epistemic and aleatory), averaged slip on the asperity (epistemic and aleatory), area of each asperity (epistemic and aleatory), slip velocity time function (epistemic), f_{max} (aleatory), rupture propagation velocity (aleatory), hypocenter (aleatory), and rupture propagation mode (aleatory).

Then, we calculated the standard deviations of the aleatory uncertainties of some of the empirical relationships of the fault parameters, which are complied in the Recipe, in order to apply these results for strong motion reproduction in past earthquakes and for strong motion prediction in future earthquakes.

Keywords: strong motion prediction, fault parameter, category, aleatory uncertainty

1. Introduction

In Japan, strong motions are often predicted by the Recipe of the Headquarters for Earthquake Research Promotion (2017, [1]), Japan, HERP hearafter. There are 27 fault parameters needed for strong motion prediction by the Recipe. The HERP classified these 27 fault parameters into 3 groups: outer fault parameters, inner fault parameters, and extra fault parameters.

In this paper, we separated fault parameters decided on assuming the seismic fault from outer fault parameters. Next, we categorized the 27 fault parameters into four groups: I) parameters defined by geological, geomorphological, or seismological investigation, II) parameters calculated by theoretical relationships with other parameters, III) parameters calculated by empirical relationships with other parameters, and IV) parameters set by assumption.

We also judged whether each parameter in the categories III and IV has an epistemic uncertainty or aleatory uncertainty.

Finally, we calculated the standard deviations of the aleatory uncertainties of some of the empirical relationships of the fault parameters, which are complied in the Recipe, in order to apply these results for strong motion reproduction is past earthquakes and for strong motion prediction in future earthquakes.

2. Fault parameters needed for strong motion prediction and their categorization

2.1 Fault parameters decided on assuming the seismic fault

Figure 1 shows the fault parameters decided when we assume the seismic fault.

1) location and geometry [Category I]

The location and the geometry of the fault are decided by the geological or geomorphological investigation. They specify the seismic source itself and make large influence on the ground motions.

2) segment for strong motion evaluation [Category I]

Segmentation for strong motion evaluation is carried out based on geological, geomorphological, or seismological investigation.

The segment for strong motion evaluation is used for asigning one or two asperities. It is the same as the geometric segment or behavioral segment, in general. However, it is different from the geometric segment when some short geometric segments are grouped as one segment for strong motion evaluation.

3) strike [Category I]

The strike is decided by geological or geomorphological investigation. It is measured clockwise from the North.

4) dip [Category I]

The dip δ is decided by geological or geomorphological investigation. It is measured from the horizontal level. Its value is hard to decide, and several values are assumed when it is not clear. Because the ground motion intensity is mainly controlled by the fault distance from the site, it gets larger on the hanging-wall sites when the dip gets smaller.

5) rake [Category I]

The rake is decided by geological, geomorphological, or seismological investigation. It is the direction of the movement of the hanging wall, and measured from the strike direction. In Japan, active faults are usually strike-slip faults or reverse faults, and oblique components are not considered. However, the ratio of the strike-slip component to the dip-slip component is considered if it can be decided by the investigation.

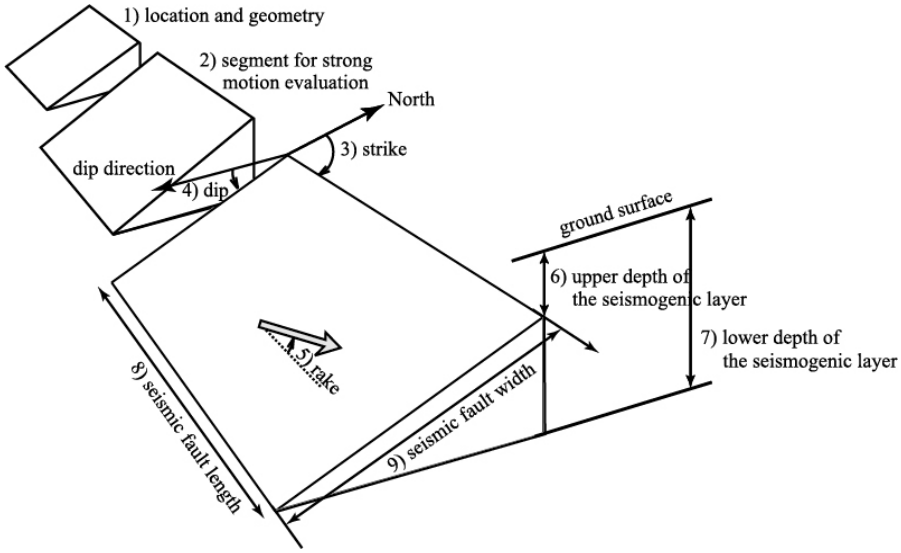

Fig. 1 – Fault parameters decided on assuming the seismic fault

6) upper depth of the seismogenic layer [Category I]

The upper depth of the seismogenic layer dep_1 is decided by the focal depths of micro-earthquakes and the underground structure. Some more cases should be considered when it is not clear. The ground motions get larger in near-fault area when the value of the upper depth gets smaller, but they hardly change in far-fault area.

7) lower depth of the seismogenic layer [Category I]

The lower depth of the seismogenic layer dep_2 is decided by the focal depths of micro-earthquakes and the underground structure. Some more cases should be considered when it is not clear. Because the lower depth of the seismogenic layer specifies the seismic fault area, other fault parameters change when the lower depth changes.

8) seismic fault length [Category I]

The seismic fault length L is decided by the location and geometry of the fault. It is the most essential parameter for decciding other parameters.

9) seismic fault width [Category II]

The seismic fault width W is calculated from the seismic fault length L for the first-stage earthquakes or from the dip δ and the upper depth dep_1 and lower depth dep_2 of the seismogenic layer for the second- and third-stage earthquakes as follows:

$$W = \begin{cases} L & (\text{for } L < W_{max}) \\ W_{max} & (\text{for } L \geqq W_{max}). \end{cases} \quad (1)$$

Here, $W_{max}=(dep_2-dep_1)/\sin\delta$.

2.2 Outer fault parameters

Figure 2 shows the outer fault parameters.

10) seismic fault area [Category II]

The seismic fault area S is calculated by the seismic fault length L and the seismic fault width W as follows:

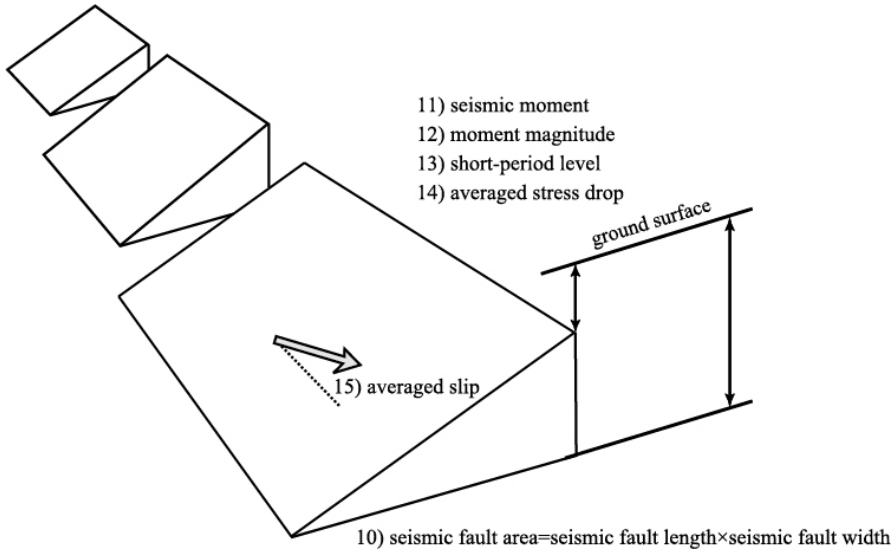

Fig. 2 – Outer fault parameters

$$S = LW. \tag{2}$$

11) seismic moment [Category III]

The seismic moment M_0 is calculated from the seismic fault area S by the empirical relationships of

$$M_0[\mathrm{N\cdot m}] = \begin{cases} \left(\dfrac{S\,[\mathrm{km}^2]}{2.23}\times 10^{15}\right)^{3/2}\times 10^{-7} & (M_0 < 7.5\times 10^{18}\,\mathrm{N\cdot m}) \\ \left(\dfrac{S\,[\mathrm{km}^2]}{4.24}\times 10^{11}\right)^{3/2}\times 10^{-7} & (7.5\times 10^{18}\,\mathrm{N\cdot m} \leqq M_0 \leqq 1.8\times 10^{20}\,\mathrm{N\cdot m}) \\ S\,[\mathrm{km}^2]\times 10^{17} & (1.8\times 10^{20}\,\mathrm{N\cdot m} < M_0). \end{cases} \tag{3}$$

The top relationship is for the first-stage earthquakes (Somerville *et al.*, 1999, [2]), the middle for the second-stage earthquakes (Irikura and Miyake, 2001, [3]), and the last for the third-stage earthquakes (Murotani *et al.*, 2014, [4]).

Recently, Tohdo *et al.* (2019, [5]) pointed out that the ruptured area above the seismogenic layer should be included in the fault area when we use equations for the second- or third-stage earthquakes.

12) moment magnitude [Category II]

The moment magnitude (Kanamori, 1977, [6]) is calculated by

$$M_W = \frac{\log M_0[\mathrm{N\cdot m}] - 7.1}{1.5}. \tag{4}$$

13) short-period level [Category III]

The short-period level A directly influences the amplitude of short-period ground motions. It is estimated from the seismic moment by the empirical relationship of Dan *et al.* (2001, [7]) as follows:

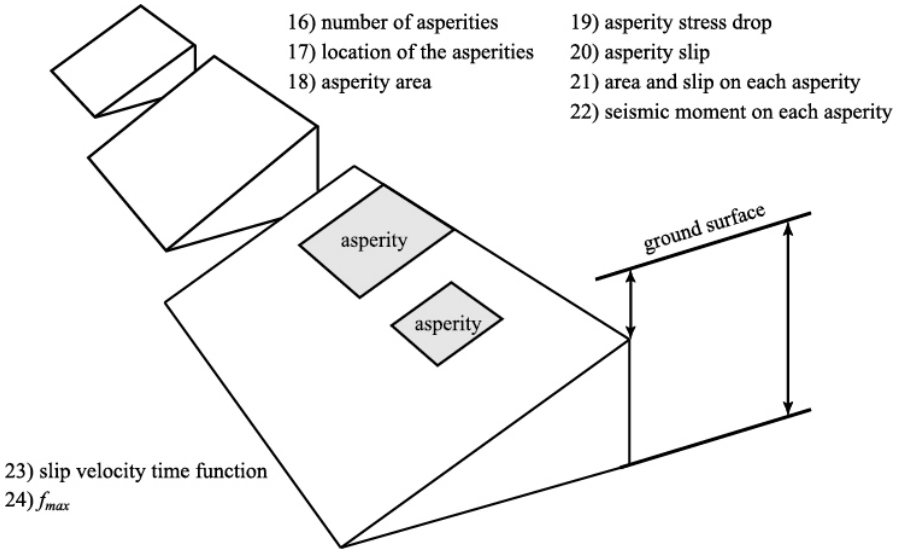

Fig. 3 – Inner fault parameters

$$A[\mathrm{N\cdot m/s^2}] = 2.46\times10^{10}\times(M_0[\mathrm{N\cdot m}]\times10^7)^{1/3}. \tag{5}$$

14) averaged stress drop [Category II]

The averaged (static) stress drop $\Delta\sigma$ is calculated from the seismic fault area S and the seismic moment M_0 by the theoretical equation of Eshelby (1957, [8]) for a buried circular crack as follows:

$$\Delta\sigma = (7/16)(\pi/S)^{3/2} M_0. \tag{6}$$

This equation can be applied to the first-stage earthquakes caused by buried faults, but not to the second- or third-stage earthquakes with surface breakings (Dan *et al*., 2019a [9]).

Irie *et al*. (2011, [10]) and Irie *et al*. (2013, [11]) proposed approximated equations for calculating the averaged dynamic stress drop for crustal earthquakes with surface breakings as follows:

$$\Delta\sigma^{\#} = c\frac{M_0}{SW}, \tag{7}$$

$$c = \begin{cases} 0.5+2\exp[-L/W] & \text{(for strike-slip faults)} \\ 0.45+0.7\exp[-L/W] & \text{(for reverse faults).} \end{cases} \tag{8}$$

Also, Dorjpalam *et al*. (2016, [12]) proposed an approximated equation for calculating the averaged dynamic stress drop for subduction plate-boundary earthquakes with surface breakings as follows:

$$c = 0.45+1.1\exp[-L/W]. \tag{9}$$

The average dynamic stress drop by equations (7) to (9) is treated to be equal to the averaged static stress drop in simulations of strong motions in past earthquakes (Dan *et al*., 2019b, [13]; Dan *et al*., 2019c [14]).

15) averaged slip [Category II]

The averaged slip D is calculated from the definition of the seismic moment M_0 by

$$D = M_0 / \mu S. \tag{10}$$

Here, μ is the rigidity at the source.

2.3 Inner fault parameters

Figure 3 shows the inner fault parameters.

16) number of asperities [Category III]

The number of the asperities is 1 or 2 in each segment for strong motion evaluation in accordance of the empirical relationship obtained by existing research papers (Somerville *et al*., 1999, [2]).

17) location of the asperities [Category I]

Sugiyama *et al*. (2002, [15]) showed that the location of the large slip areas on the fault in the seismogenic layer corresponds to the location of large displacement of the surface faults. Hence, the asperities are assigned to the place with relatively large displacement per event or cumulative displacement of the active fault. In case of unclear active faults, the asperities are assigned to the place of a clearer fault. In case of the strong motion prediction at a specific site, it is recommended to assign the asperity to the place closest to the site within the appropriate range because the distance from the asperity to the site controls the amplitude of the motions.

18) asperity area [Category II]

The asperity fault area S_{asp} is calculated from the seismic fault area S, the averaged stress drop $\Delta\sigma$, and the short-period level A by

$$S_{asp} = \pi(4\beta^2 S\Delta\sigma / A)^2. \tag{11}$$

Note here that the asperity area S_{asp} becomes too large for long faults, which can not be modeled by a buried circular crack, and that other stress drop equations (*e.g*., Irie *et al*., 2011, [10]; Irie *et al*., 2013, [11]; Dorjpalam *et al*., 2016, [12]) should be applied.

19) asperity stress drop [Category II]

The asperity stress drop $\Delta\sigma_{asp}$ is calculated from the short-period level A, the seismic fault area S, and the averaged stress drop $\Delta\sigma$ by

$$\Delta\sigma_{asp} = A^2 / (16\pi\beta^4 S\Delta\sigma). \tag{12}$$

20) asperity slip [Category III]

The asperity slip D_{asp} is usually set by the empirical relationship of Somerville *et al*. (1999, [2]) as follows:

$$D_{asp} = 2D. \tag{13}$$

When we know the displacement per event D_{surf} by active fault investigation, the asperity slip D_{asp} can be changed because Matsushima *et al*. (2010, [16]) obtained the following empirical relationship:

$$D_{surf} = (2\sim3)\times D = (1\sim1.5)\times D_{asp}. \tag{14}$$

21) area and slip on each asperity [Category III]

In case of two asperities in one segment for strong motion evaluation, each asperity area S_{aspi} is decided by the area ratio of 16:6 (Somerville *et al*., 1999, [2]). The averaged slip on each asperity is distributed proportionally to the square root of each asperity area S_{aspi}, because this gives the apparently constant stress drop to the segments by equation (6).

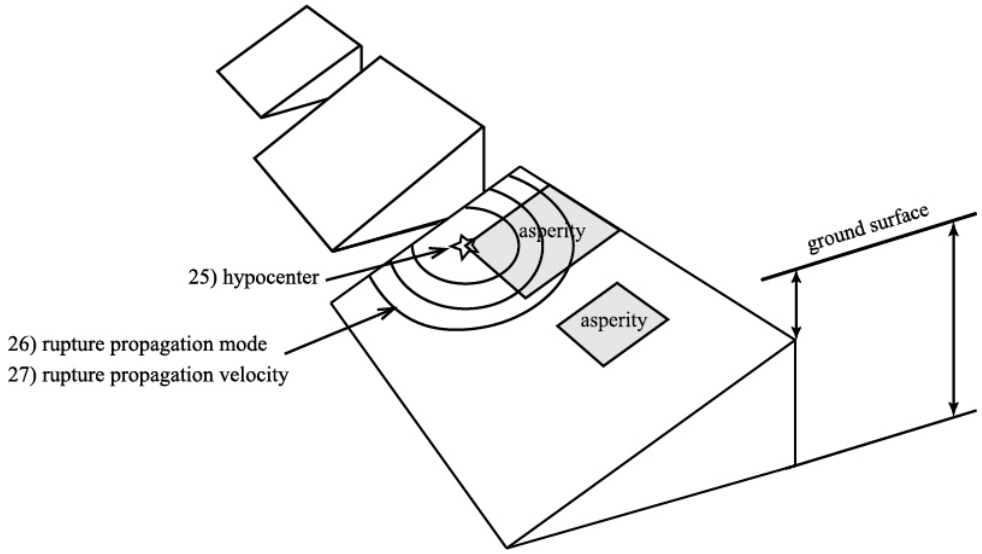

Fig. 4 – Extra fault parameters

22) seismic moment on each asperity [Category II]

The seismic moment on each asperity M_{0i} is calculated from the asperity slip D_{aspi} and asperity area S_{aspi} by

$$M_{0i} = \mu D_{aspi} S_{aspi}. \tag{15}$$

23) slip velocity time function [Category III]

The approximated slip velocity time function proposed by Nakamura and Miyatake (2000, [17]) is used so far in the theoretical method such as the wavenumber integration technique. It was obtained by the dynamic fault rupturing simulation, and it is necessary to improve the short-period components of the slip velocity time function. In practice, the short-period components of the ground motions are predicted by the empirical Green's function method or the stochastic Green's function method.

24) f_{max} [Category III]

Ground motions of frequencies higher than the f_{max} are proportional to the square of the f_{max}. Several values are proposed: 6 Hz (Tsurugi *et al*., 1997, [18]), 13.5 Hz (Satoh *et al*., 1994, [19]), and 8.3 Hz (Kagawa *et al*., 2003, [20]). Its value should be validated by comparing the predicted ground motions with records or GMPE's (Ground Motion Prediction Equations).

2.4 Extra fault parameters

Figure 4 shows the extra fault parameters.

25) hypocenter [Category IV]

The duration of the motion gets shorter and the amplitude gets larger at the points where the fault rupture front approaches, and the duration gets longer and the amplitude gets smaller at the points where the fault rupture front gets away. The location of the hypocenter influences the ground motions, especially strong motion pulses. We can sometimes estimate some candidates of the location of the hypocenter by geometry of the fault branchings (Nakata *et al*., 1998, [21]). However, in general, it is hard to decide the location and we have to assume several locations in practice.

26) rupture propagation mode [Category IV]

The rupture propagation mode in the actual natural earthquakes is not simple, but a circular mode (constant rupture propagation velocity) is often assumed in the strong motion prediction.

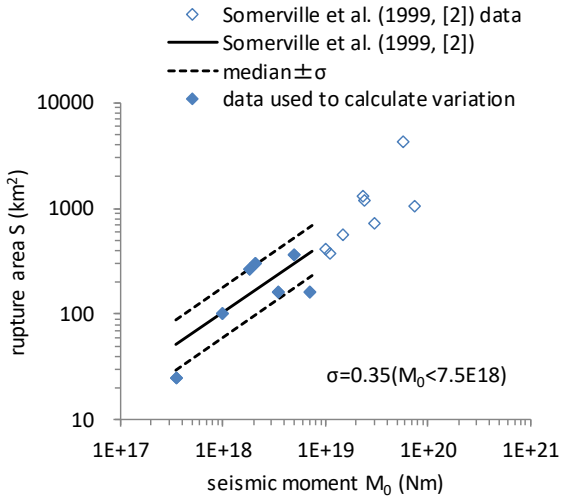

Fig. 5 – Relationship between the seismic moment and ruptured area from Somerville *et al.* (1999, [2])

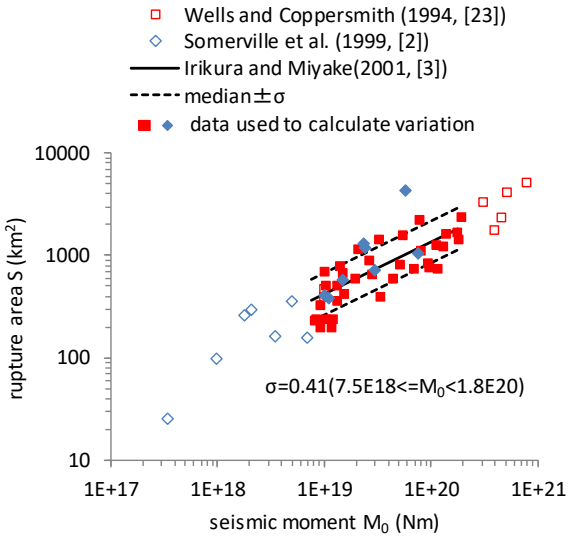

Fig. 6 – Relationship between the seismic moment and ruptured area from Irikura and Miyake (2001, [3])

27) rupture propagation velocity [Category IV]

The rupture propagation velocity v_r affects the amplitude of the strong motion pulses with a period of about 1 second at the points near the fault trace. The value of the rupture propagation velocity v_r is often assumed according to Geller (1976, [22]) as follows:

$$v_r = 0.72\beta. \tag{16}$$

Here, β is the *S*-wave velocity at the source. Its variation should be considered in practice.

3. Epistemic and aleatory uncertainties

We also judged whether each parameter in the categories III and IV has an epistemic uncertainty or aleatory uncertainty as follows: seismic moment (epistemic and aleatory), short-period level (epistemic and aleatory), averaged slip on the asperity (epistemic ad aleatory), area of each asperity (epistemic and aleatory), slip velocity time function (epistemic), f_{max} (aleatory), rupture propagation velocity (aleatory), hypocenter (aleatory), and rupture propagation mode (aleatory).

4. Standard deviation of the aleatory uncertainties

We calculated the standard deviations of the aleatory uncertainties of some of the empirical relationships of the fault parameters, which are complied in the Recipe, in order to apply these results for strong motion reproduction in past earthquakes and for strong motion prediction for future earthquakes.

1) seismic moment

The seismic moment M_0 is calculated from the fault area S as shown in equation (3), and the range of the seismic moment is described for each of the first, second, and third stages.

For first-stage earthquakes, we compiled the database in Somerville *et al.* (1999, [2]), and obtained

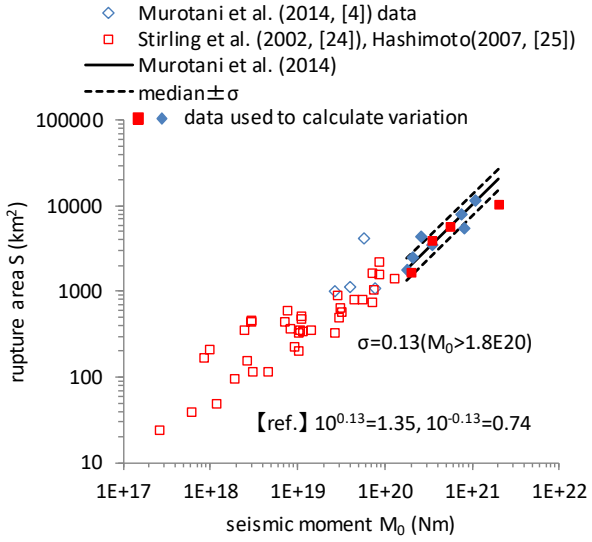

Fig. 7 – Relationship between the seismic moment and ruptured area from Murotani *et al.* (2014, [4])

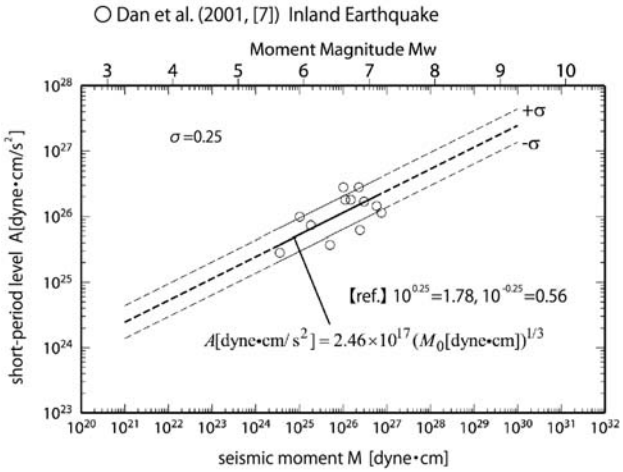

Fig. 8 – Relationship between the seismic moment and short-period level from Dan *et al.* (2001, [7])

$$\log M_0\,[\mathrm{N\cdot m}]=(3/2)\log(S\,[\mathrm{km}^2]/2.23)-7\pm0.35. \tag{17}$$

Figure 5 shows the data and the above relationship with the standard deviation. We used the solid square data ($M_0<7.5\times10^{18}$ N·m) for the calculation.

For second-stage earthquakes, we compiled the database in Irikura and Miyake (2001, [3]), and obtained

$$\log M_0\,[\mathrm{N\cdot m}]=2\log(S\,[\mathrm{km}^2]\times10^{11}/4.24)-7\pm0.41. \tag{18}$$

Figure 6 shows the data and the above relationship with the standard deviation. We used the solid square data (7.5×10^{18} N·m$\leqq M_0\leqq1.8\times10^{20}$ N·m) for the calculation.

For third-stage earthquakes, we compiled the database in Murotani *et al.* (2014, [4]), and obtained

$$\log M_0[\mathrm{N\cdot m}]=\log S\,[\mathrm{km}^2]+17\pm0.13. \tag{19}$$

Figure 7 shows the data and the above relationship with the standard deviation. We used the solid square data (1.8×10^{20} N·m$<M_0$) for the calculation.

2) short-period level

We used the database in Dan *et al.* (2001, [7]), and obtained

$$\log A[\mathrm{N\cdot m/s}^2]=\log(2.46\times10^{10})+(1/3)\log M_0[\mathrm{N\cdot m}]+7\pm0.25. \tag{20}$$

Figure 8 shows the data and the above relashionship with the standard deviation.

3) averaged slip on the asperity

We used the database by Somerville *et al.* (1999, [2]), and obtained

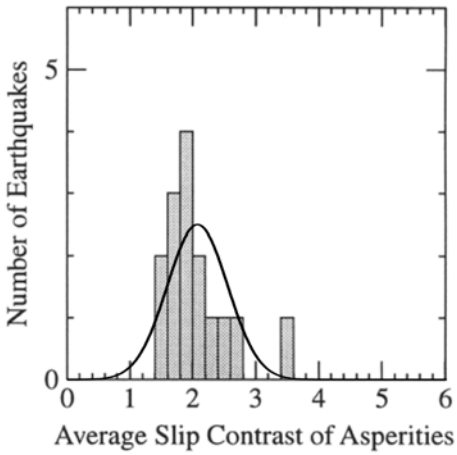

Fig. 9 – Histogram of the average slip contrast of asperities from Somerville *et al*. (1999, [2])
The authors added probability density function to Somerville's histogram.

Table. 1 – Ratio of the rupture propagation velocity to the *S*-wave velocity from Geller (1976, [22])

No.	Event	Ms	*Vr* (km/s)	type*	β (km/s)	Vr/β
2	1927 Tango	7.75	2.3	c	3.5	0.66
4	1933 Saitama	6.75	2.3	c	3.5	0.66
5	1933 Sanriku	8.3	3.2	l	4.5	0.71
6	1933 Long Beach	6.25	2.3	c	3.5	0.66
8	1943 Tottori	7.4	2.3	c	3.5	0.66
12	1948 Fukui	7.3	2.3	c	3.5	0.66
16	1960 Chile	8.3	3.5	l	4.5	0.78
17	1961 Kitamino	7.0	3.0	c	3.5	0.86
18	1963 Wakasa Bay	6.9	2.3	c	3.5	0.66
20	1963 Kurile Islands	8.2	3.5	l	4.5	0.78
22	1964 Spain	7.1	1.4	c	3.5	0.40
23	1964 Alaska	8.5	3.5	l	4.5	0.78
25	1965 Rat islands I	7.9	4.0	l	4.5	0.89
27	1966 Parkfield	6.4	2.7	c	3.5	0.77
32	1968 Tokachi-Oki	8.0	3.5	l	4.5	0.78
33	1968 Saitama	5.8	3.4	c	3.5	0.97
35	1969 Kurile Islands	7.8	3.5	l	4.5	0.78
36	1969 Gifu	6.6	2.5	c	3.5	0.71
37	1970 Peru	7.8	2.5	l	4.5	0.56
38	1971 San Fernando	6.6	2.4	c	3.5	0.69
					mean	0.72±0.12

* c: shallow crustal events, l: events breaking the entire lithosphere (subduction plate-boundary earthquakes)

$$D_{asp} / D = 2.0 \pm 0.48. \quad (21)$$

Figure 9 shows the histogram of the averaged slip contrast of asperities and the above relationship with the one standard deviation.

4) rupture propagation velocity

We used the database of the rupture propagation velocity in Geller (1976, [22]), and obtained

$$V_r = (0.72 \pm 0.12)\beta. \quad (22)$$

Table 1 lists the ratio of the wave propagation velocity to the *S*-wave velocity.

5. Conclusions

We categorized 27 fault parameters used for strong motion prediction into four groups as follows:

I) parameters defined by geological, geomorphological, or seismological investigation,

II) parameters calculated by theoretical relationships with other parameters,

III) parameters calculated by empirical relationships with other parameters,

IV) parameters set by assumption.

We also judged whether each parameter in the categories III and IV has an epistemic uncertainty or aleatory uncertainty as follows: seismic moment (epistemic and aleatory), short-period level (epistemic and aleatory), averaged slip on the asperity (epistemic and aleatory), area of each asperity (epistemic and aleatory), slip velocity time function (epistemic), f_{max} (aleatory), rupture propagation velocity (aleatory), hypocenter (aleatory), and rupture propagation mode (aleatory).

Then, we calculated the standard deviations of the aleatory uncertainties of some of the empirical relationships of the fault parameters, which are complied in the Recipe, in order to apply these results for strong motion reproduction in past earthquakes and for strong motion prediction in future earthquakes.

6. References

[1] Headquarters for Earthquake Research Promotion (2017): Strong ground motion prediction method for earthquakes with specified source faults (“Recipe”).

[2] Somerville PG, Irikura K, Graves R, Sawada S, Wald D, Abrahamson N, Iwasaki Y, Kagawa T, Smith N, Kowada A (1999): Characterizing crustal earthquake slip models for the prediction of strong ground motion. *Seismological Research Letters*, **70** (1), 59-80.

[3] Irikura K, Miyake H (2001): Prediction of strong ground motions for scenario earthquakes. *Journal of Geography*, 110, 849-875 (in Japanese with English abstract).

[4] Murotani S, Matsushima S, Azuma T, Irikura K, Kitagawa S (2014): Scaling relations of source parameters of earthquakes occurring on inland crustal mega-fault systems. *Pure and Applied Geophysics*, DOI10.1007/s00024-014-1010-9.

[5] Tohdo M, Oana A, Dan K (2019): Effects of different ways of counting fault area for asperity model of crustal earthquakes on fault parameters and predicted strong ground motions. *Journal of Japan Association for Earthquake Engineering*, **19** (3), 22-37.

[6] Kanamori H (1977): The energy release in great earthquakes. *Journal of Geophysical Research*, **82** (20), 2981-2987.

[7] Dan K, Watanabe M, Sato T, Ishii T (2001): Short-period source spectra inferred from bariable-slip rupture model s and modeling of earthquake faults for strong motion prediction by semi-empirical method. *Journal of the Structural and Construction Engineering (Transactions of the Architectural Institute of Japan)*, **545**, 51-62.

[8] Eshelby, JD (1957): The determination of the elastic field of an ellipsoidal inclusion, and related problems. *Proceedings of the Royal Society of London*, Series A (241), 376-396.

[9] Dan K, Tohdo M, Oana A (2019a): Examination of averaged stress drop equations connecting outer and inner fault parameters for strong motion prediction. *Journal of Japan Association for Earthquake Engineering*, **19** (5), 96-110.

[10] Irie K, Dan K, Dorjpalam S, Kawasato T, Ikutama S, Irikura K (2011): Procedure for establishing asperity models for long strike-slip faults based on change in scaling laws of fault parameters. Part 3: Estimation of the formula for average dynamic stress drop by dynamic rupturing simulation. *Summaries of Technical Papers of Annual Meeting, Architectural Institute of Japan*, 103-104 (in Japanese).

[11] Irie K, Dan K, Torita H, Kase Y (2013): Estimation of dynamic stress drops of inland earthquakes caused by long reverse faults. *Proc. of the 10th Annual Meeting of Japan Association for Earthquake Engineering*, 375-376 (in Japanese).

[12] Dorjpalam S, Dan K, Ju D, Irie K (2016): Examination of the geometric constant in the average dynamic stress drop equation for long thrust faults by dynamic rupture simulation, Part 5: Simulation results for a layered medium. *Summaries of Technical Papers of Annual Meeting, Architectural Institute of Japan*, 1135-1136.

[13] Dan K, Ju D, Fujiwara H, Morikawa N (2019b): Validation of the new procedures for evaluating parameters of crustal earthquakes caused by long faults for ground motion prediction, *Bulletin of the Seismological Society of America*, **109** (1), 152-163.

[14] Dan K, Oana a, Fujiwara H, Morikawa N (2019c): Extension of the procedure for evaluating parameters of strike-slip fault with surface breakings for strong motion prediction, *Proceedings of the 7th International Conference on Earthquake Geotechnical Engineering*, 1952-1960.

[15] Sugiyama Y, Sekiguchi H, Awata Y, Fusejima Y, Shimokawa K (2002): Relationship between active fault information and heterogeneous source characteristics, Report of Master Model for Strong Motion Prediction for Earthquake Disaster Mitigation, 119-129.

[16] Matsushima S, Murotani S, Azuma T, Irikura K, Kitagawa S (2010): Scaling relations of earthquakes on active mega-fault systems. *Geophysical Bulletin of Hokkaido University*, **73**, 117-127 (in Japanese with English abstract).

[17] Nakamura H, Miyatake T (2000): An approximate expression of slip velocity time function for simulation of near-field strong ground motion. *Journal of the Seismological Society of Japan*, **2** (53), 1-9 (in Japanese).

[18] Tsurugi M, Kagawa T, Irikura K, Kowada A (1997): Cutoff frequency f_{max} of earthquakes occurring in Kinki distinct. *Abstracts of the Japan Earth and Planetary Science Joint Meeting*, 103 (in Japanese).

[19] Satoh T, Kawase H, Sato T (1994): Statistical spectral characteristics for engineering bedrock waves in which local site effects of surface geology are removed. *Journal of the Structural and Construction Engineering (Transactions of the Architectural Institute of Japan)*, 462, 79-89 (in Japanese).

[20] Kagawa T, Tsurugi M, Sato N (2003): A study on high frequency cut-off characteristics of strong ground motion records observed at hard sites. *Japan Society of Civil Engineering, Journal of Earthquake Engineering*, 1-4 (in Japanese).

[21] Nakata T, Shimazaki K, Suzuki Y, Tsukuda E (1998): Fault branching and directivity of rupture propagation. *Journal of Geography*, **107** (4), 512-528 (in Japanese).

[22] Geller R (1976): Scaling relations for earthquake source parameters and magnitudes. *Bulletin of the Seismological Society of America*, **66** (5), 1501-1523.

[23] Wells DL, Coppersmith KJ (1994): New Empirical Relationships among Magnitude, Rupture Length, Rupture Width, Rupture Area, and Surface Displacement, *Bulletin of the Seismological Society of America*, **84** (4), 974-1002.

[24] Stirling M, Rhoades D, Berryman K (2002): Comparison of Earthquake Scaling Relations Derived from data of the Instrumental and Preinstrumental Era, *Bulletin of the Seismological Society of America*, **92** (2), 812-830.

[25] Hashimoto T (2007): The surface length of earthquake fault and the moment magnitude, *Proceedings of Japan Geoscience Union Meeting*, S145-013 (in Japanese).

